15th Triennial World Congress, Barcelona, Spain

FORMATION CONTROL OF MULTIPLE AUTONOMOUS VEHICLES: THEORY AND EXPERIMENTATION[1]

Wei Kang*, Ning Xi†, Yiwen Zhao‡, Jindong Tan†, Yuechao Wang‡

*Mathematics Department, Naval Postgraduate School,
Monterey, CA 93943
†Department of ECE, Michigan State University,
East Lansing, MI 48824.
‡ Shenyang Institute of Automation, Chinese Academy of Science
Shenyang, P.R. China

Abstract: The formation control of multiple vehicles using a perceptive frame is studied in this paper. The method is applied to multiple mobile robots. The controller design and lab experiments are shown in the paper. Some useful strategies of coordination are implemented in a perceptive frame by reference projections. The feature of the coordination is illustrated by experiments of three mobile robots.

Keywords: Control system design, control algorithms, control applications, mobile robots

1 INTRODUCTION[1]

In (Kang, et al ., 2000), the control design in a *perceptive frame* was developed for the formation of multiple autonomous vehicles. Using the design method, controllers can be found to keep multiple vehicles in a required formation, and to coordinate the vehicles in the presence of environmental changes. The model adopted in (Kang, et al ., 2000) is a general dynamical system of ordinary differential equations. The method is applicable to general autonomous vehicles. In this paper, we apply the controller designed in a perceptive frame to the formation of multiple ground vehicles. Lab experiment results are reported in this paper. The experimental results clearly illustrate the advantages of the formation controller in a perceptive frame.

In section 2, the formation of general dynamical systems is defined. Then, the controller design in a perceptive frame is summarized in a simple four-step algorithm. In section 3, several coordination strategies are studied for multiple ground vehicles. In section 4, the coordinated formation controllers are implemented in three holonomic mobile robots. The lab experimental results are shown. They clearly illustrate the advantages of the coordinated controller developed in this paper.

2 FORMATION AND CONTROLLER DESIGN ALGORITHM

2.1 Formation and Action Reference

The model of a complex system with multiple subsystems (vehicles) is given by the following equations

$$\frac{dx_i}{dt} = f_i(x_i, u_i, r_i), y_i = h_i(x_i), \quad 1 \le i \le k \quad (1)$$

where k is the total number of subsystems. The variable $x_i \in \mathbb{R}^{n_i}$ is the state of the ith subsystem. The function r_i represents the coupling of subsystems. It is a function of (x_j, u_j) for $j \neq i$. The input $u_i \in \mathbb{R}^{m_i}$ is the control variable for the ith subsystem. The output function $h_i(x_i)$ represents the performance. For instance, for the formation of multiple ground vehicles, h_i represents the position of the ith vehicle. For the formation of multiple robot manipulators moving an object, h_i represents the force exerted on the object and the position of the ith manipulator. We assume that $y_i \in \mathbb{R}^p$, where p is a constant for all subsystems.

A *formation* is defined in a coordinate frame, which moves with the desired trajectory. Let $y_d(s)$ be any curve in $\mathbb{R}^p$ with parameter s. Let $\mathcal{F}(s) = \left[\ \mathbf{e}_1(s), \ \ \mathbf{e}_2(s), \ \ \cdots, \mathbf{e}_p(s) \ \right]$ be p orthonormal vectors in $\mathbb{R}^p$ which forms a moving frame. The origin of the moving frame is $y_d(s)$. A formation consists of k points in $\mathcal{F}$, denoted by $F = \{P_1, P_2, \cdots, P_k\}$, where $P_i = \sum_{j=1}^{p} \alpha_{ij}\mathbf{e}_j$. If α_{ij} is a function of s or time t, the formation is time-variant. Otherwise, the formation is time-

[1] Research supported in part by NSF IRI 9796287, NSF IRI 9796300.

invariant.

The concept *action reference* is a key parameter determined by the task of a control problem. In the formation control problem, a convenient choice for action reference is s, the parameter used for the desired path $y_d(s)$. How to compute the value of action reference using sensor information is discussed in § 2.2 using reference projections. The projection converts the sensory information into the value of the action reference, then the value of s is converted to the synthetic time which is used to coordinate the lower level feedbacks.

2.2 Control Law Design and the Reference Projection

In this section, we introduce the design method of formation control developed in (Kang, et al ., 2000). The controller design in a perceptive frame has the following four steps.

The first step is to generate the desired path for each subsystem in the formation. Given a desired path $y_d(s)$, and given a formation $\{P_1, \cdots, P_k\}$ in the moving frame $\mathcal{F}$, the path for each subsystem is generated by

$$y_{di}(s) = y_d(s) + \sum_{j=1}^{p} \alpha_{ij} \mathbf{e}_j(s) \qquad (2)$$

The action reference is the parameter s. The speed of the formation moving along $y_d(s)$ is determined by the task. It is defined by a strictly increasing function

$$s = v(t).$$

A formation control law is a feedback $u = \alpha(x)$ which satisfies

$$\lim_{t\to\infty} (y_i(t) - y_{di}(v(t))) = 0. \qquad (3)$$

Furthermore, if the initial position is on the desired path, then the trajectory of the controlled system follows the path. More specifically, there exists an initial condition of the system $x_0 = (x_{01}, x_{02}, \cdots, x_{0k})^T$ such that the trajectory starting from x_0 satisfies $h_i(x(t)) = y_{di}(t)$. Denote this path by $x_{di}(s)$ or $x_{di}(v(t))$.

The second step in the controller design is to find control laws for subsystems. They might be time varying feedbacks. The control law $u_i = \alpha_i(x, t)$, $1 \leq i \leq k$, for each subsystem is designed separately using any existing method of signal tracking or path following. Two subsystems may adopt different control design algorithms.

Theoretically, the control laws $u_i = \alpha_i(x, t)$ can drive the system move in formation along y_d because they are designed to satisfy (3). However, the feedbacks are designed separately. There is no coordination between the subsystems. To improve the performance and coordination of the feedback, a projection mapping is introduced in the next step.

The third step is to define the *reference projection.* The projection is a transformation $s = \gamma(x)$ satisfying

$$\gamma(x_d(s)) = s \qquad (4)$$

i.e. if the state is on the desired path, γ should give the corresponding value of s on the desired trajectory $x_d(s)$. For example, given any state x_0, let $x_d(s_0)$ be the orthogonal projection from x_0 to $x_d(s)$. If we define $\gamma(x_0) = s_0$, then it satisfies (4). However, orthogonal projection is not the only way to define γ. It is shown in section 3 that changing the projection transformation γ can fundamentally change the way subsystems coordinated with each other.

The last step of the controller design is to construct a non-time based feedback law, which is used to control the system of multiple vehicles. The process is simply a substitution. The control law is given by

$$\alpha_i(x) = \alpha_i(x, v^{-1}(\gamma(x))) \qquad (5)$$

Notice that the time t is replaced by the perceptive or synthetic time, $v^{-1}(\gamma(x))$. The closed-loop system with non-time based feedback is

$$\dot{x}_i = f_i(x, \alpha_i(x)). \qquad (6)$$

Mission tasks and coordination requirements determine which reference projection to be adopted. How to defined a projection reflecting the coordination requirement of a mission is discussed in § 3.

The stability of the closed-loop system could be changed by the reference projection, as it was pointed out in (Kang, et al ., 2000). It was also proved in (Kang, et al ., 2000) that if the derivative of the perceptive time $v^{-1}(\gamma(x))$ approaches 1, the stability of the system with the reference projection is guaranteed. In the simulations and experiments that follow, systems with reference projections are stable.

2.3 An Example of Wedge Formation

In the following, an example of tracking in formation is given to illustrate the design method developed in § 2.2. The problem is to drive three nonholonomic cars to form a wedge, and to follow a sine curve in the xy-plane.

Formation: In the moving frame $\mathcal{F}$, the wedge formation is defined by the three points: $P_1 =$ the origin of $\mathcal{F}$, $P_2 = -d_1\mathbf{e}_1 + d_2\mathbf{e}_2$ and $P_3 =$

$-d_1\mathbf{e}_1 - d_2\mathbf{e}_2$. The numbers d_1 and d_2 are positive.
Path of the formation: The path is given by the parametric equations

$$x_d = s, \quad y_d = \sin s. \tag{7}$$

$\mathbf{e}_1$ of the moving frame $\mathcal{F}$ is tangent to (x_d, y_d),

$$\begin{aligned} \mathbf{e}_1 &= \frac{1}{\sqrt{1+\cos^2 s}} \begin{bmatrix} 1 & \cos s \end{bmatrix}^T \\ \mathbf{e}_2 &= \frac{1}{\sqrt{1+\cos^2 s}} \begin{bmatrix} -\cos s & 1 \end{bmatrix}^T. \end{aligned} \tag{8}$$

Velocity: We define $s = v(t) = t$.
Desired trajectories for each subsystem: The trajectories of the vehicles are given by (2). More specifically

$$\begin{aligned} & x_{d1} = t, \quad y_{d1} = \sin t \\ & x_{d2} = t + \frac{-d_1 - d_2\cos t}{\sqrt{1+\cos^2 t}}, y_{d2} = \sin t + \frac{-d_1\cos t + d_2}{\sqrt{1+\cos^2 t}} \\ & x_{d3} = t + \frac{-d_1 + d_2\cos t}{\sqrt{1+\cos^2 t}}, y_{d3} = \sin t + \frac{-d_1\cos t - d_2}{\sqrt{1+\cos^2 t}} \end{aligned} \tag{9}$$

Low-level feedback: The control feedback of a vehicle is from (Kang and Xi, 1999). The model of a vehicle is

$$\begin{aligned} \dot{x}_i &= u_i\cos\theta_i, \quad \dot{y}_i = u_i\sin\theta_i \\ \dot{\theta}_i &= \frac{u_i}{l} tan\phi_i, \quad \dot{\phi}_i = v_i, \end{aligned} \tag{10}$$

where u_i corresponds to the forward velocity of the rear wheels of the car and v_i corresponds to the velocity of the steering wheel, the angle of the car body with respect to the horizontal is θ_i, the steering angle with respect to the car body is ϕ_i, (x_i, y_i) is the location of the rear wheels, l is the length between the front and the rear wheels. Given the desired path, The feedback of u_i and v_i are

$$u_i(x_i, y_i, \theta_i, \phi_i, t) = \frac{1}{\cos\theta_i}(\dot{x}_{di} - (x_i - x_{di})). \tag{11}$$

$$v_i = -\frac{\alpha_2 - \alpha_1 - u_i(a_1e_1 + a_2e_2 + a_3e_3)}{\beta_2(x_i, y_i, \theta_i, \phi_i, t) - \beta_1(\theta_i, \phi_i)}, \tag{12}$$

where

$$\begin{aligned} & \alpha_1(\theta_i, \phi_i) = -\frac{1}{l^2}\sin\theta_i(\tan\phi_i)^2, \quad \beta_1(\theta_i, \phi_i) = \frac{\cos\theta_i}{l\cos^2\phi_i} \\ & e_1 = y_i - y_{di}, \quad e_2 = \sin\theta_i - \frac{\dot{y}_{di}}{u_i}, \\ & e_3 = \frac{1}{l}\cos\theta_i\tan\phi_i - \frac{1}{u_i}\frac{d}{dt}(\frac{\dot{y}_{di}}{u_i}), \\ & \alpha_2(x_i, y_i, \theta_i, \phi_i, t) + \beta_2(x_i, y_i, \theta_i, \phi_i, t)v \\ & = \frac{d}{dt}(\frac{1}{u_i}\frac{d}{dt}(\frac{\dot{y}_{di}}{u_i})). \end{aligned}$$

Reference projection: In this example, $\gamma(x, y, \theta, \phi) = x_1$. This projection implies that the first car leads the formation. More reference projections will be given in § 3 to implement different kinds of coordination strategies.

The feedback (11)-(12) is time dependent. The final lower level feedbacks are obtained by substituting $t = v^{-1}(\gamma)$ into (11)-(8), i.e. $u_i = u_i(x_i, y_i, \theta_i, \phi_i, x_1)$ and $v_i = v_i(x_i, y_i, \theta_i, \phi_i, x_1)$. The simulations show that the three car moves along the sine curve in the wedge formation. In the simulation, $d_1 = 0.25, d_2 = 0.5, l = 0.25$. The initial location of the vehicles are $(0, 0)$, $(-0.4, 0.3)$, and $(-0.2, -0.4)$ for P_1, P_2 and P_3 respectively. In Figure 1, the three curves are the path of the three vehicles. The formations at $t = 3\pi/4$, $t = 3\pi/2$ and $t = 2\pi$ are shown in the plot.

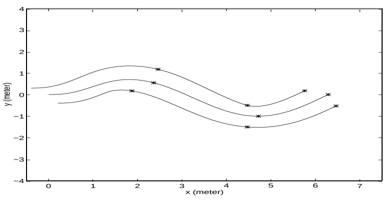

Figure 1: The path of the vehicles in the wedge formation

3 REFERENCE PROJECTION AND COORDINATION STRATEGY

It is shown in the previous section that the time variable t or the action reference s in the control feedback can be substituted by the reference projection to achieve a time invariant control law. It makes the feedback completely autonomous. Furthermore, the reference projection that does the job is not unique. In the formation control of multiple vehicles, the freedom in the selection of reference projections is an advantage that we take to achieve coordination among the vehicles. In the following, we introduce several useful reference projections that follow a variety of coordination strategies.

Suppose three vehicles R1, R2 and R3 move in formation. Define the reference projection by

$$\gamma(x) = x_1,$$

where x_1 is the x coordinate of R1. Under this projection, R1 is the team leader. If R1 slows down, then the entire formation will slow down. If R1 recovers the desired path, the entire formation will automatically recover the desired formation. So, the reference projection defines a *movement with a leader.*

Another coordination strategy is the *simultaneous movement.* Under this strategy, all vehicles slow down or stop if any vehicle in the formation slows down or stops. In other words, the entire formation slows down or stops simultaneously. There is no team leader who set up the speed. The reference projection that realizes the simultaneous movement is

$$\gamma(x) = min(x_1 - d_1, x_2, x_3) + d_1. \quad (13)$$

In this projection, the vehicle left behind defines the value of the action reference s.

In the *series connection of formations*, the kth vehicle is the leader of the $(k+1)$th vehicle. If the kth vehicle slows down or stops, the jth vehicle with $j > k$ has to slow down or stop to avoid collision. However, the jth vehicle with $j < k$ may keep moving. To follow the above coordination strategy, we define $\gamma_1(x) = x_1$, $\gamma_2(x) = x_1 - d$, $\gamma_3 = x_2 - d$, etc. In general, $\gamma_i = x_{i-1} - d$. Different from the movement with a leader or simultaneous movement, string instability is a potential problem in the series connection. A possible solution is to define γ_i by the average position of several cars in front, or to use more sensory information such as the acceleration of the leading vehicle.

4 EXPERIMENTAL RESULTS

In this section, a series of experimental results are shown to test the formation control algorithm developed in the previous sections. The experiments are carried out using three mobile holonomic omnidirection robots, denoted by R1, R2, and R3. The robots report their positions to a station PC every 100ms. Then the station PC calculates the velocity of the robots using a control law in a perceptive frame. The control value is send to each robot as a command. The robots have sonar sensors. The robot will stop when obstacles are detected by the sonar sensor. In the experiment, we only use the sonar of the leader robot R1.

4.1 Movement with a Leader

In this experiment, we use the wedge formation of three vehicles, the same formation as in § 2.3. The parameters in the formation are $d_1 = 1000mm$, and $d_2 = 600mm$. The desired path of the leader, R1, and the moving frame are defined by

$$x = s, y = k_1 \sin(k_2 s), k_1 = 500mm, k_2 = \frac{\pi}{3000}$$
$$\mathbf{e}_1 = \frac{1}{\sqrt{1+\cos^2 k_2 s}} \begin{bmatrix} 1 & \cos k_2 s \end{bmatrix}^T$$
$$\mathbf{e}_2 = \frac{1}{\sqrt{1+\cos^2 k_2 s}} \begin{bmatrix} -\cos k_2 s & 1 \end{bmatrix}^T.$$

The desired trajectories for R2 and R3 are

$$x_{d2} = s + \frac{-d_1 - d_2 \cos k_2 s}{\sqrt{1+\cos^2 k_2 s}},$$
$$y_{d2} = k_1 \sin k_2 s + \frac{-d_1 \cos k_2 s + d_2}{\sqrt{1+\cos^2 k_2 s}}$$
$$x_{d3} = s + \frac{-d_1 + d_2 \cos k_2 s}{\sqrt{1+\cos^2 k_2 s}},$$
$$y_{d3} = k_1 \sin k_2 s + \frac{-d_1 \cos k_2 s - d_2}{\sqrt{1+\cos^2 k_2 s}}$$

Different from § 2.3, the desired velocity is defined by a constant speed $V = 100mm/s$. therefore,

$$\dot{x}_{d1}^2 + \dot{y}_{d1}^2 = V^2.$$

The desired velocities of the mobile robots are

$$\dot{x}_{di} = \frac{V}{\sqrt{K(s)}} \left(1 + k_2 \frac{d_{yi}\sqrt{K(s)} \sin k_2 s}{K(s)\sqrt{K(s)}} - k_2 \frac{(d_{yi} \cos k_2 s - d_{xi}) \sin k_2 s \cos k_2 s}{K(s)\sqrt{K(s)}} \right),$$
$$\dot{y}_{di} = \frac{V}{\sqrt{K(s)}} \left(\cos k_2 s - k_2 \frac{(d_{xi}\sqrt{K(s)} \sin k_2 s}{K(s)\sqrt{K(s)}} - k_2 \frac{(d_{xi} \cos k_2 s + d_{yi}) \sin k_2 s \cos k_2 s}{K(s)\sqrt{K(s)}} \right).$$

where $K(s) = 1 + \cos^2 k_2 s$, $d_{x1} = d_{y1} = 0$, $d_{x2} = -1000$, $d_{y2} = 600$, $d_{x3} = -1000$, $d_{y3} = -600$. Since the vehicle is holonomic, the control of x and y follows a simple linear control law

$$\ddot{x}_i = k_d(x_{di} - x_i) + k_v(\dot{x}_{di} - \dot{x}_i)$$
$$\ddot{y}_i = k_d(y_{di} - y_i) + k_v(\dot{y}_{di} - \dot{y}_i).$$

Each individual control depends on the action reference s. We define the reference projection by $s = x_1$. It implies that the formation leader is R1. The value of x_1 is obtained by the real-time measurement of R1. Several experiments were carried out using different values of k_d and k_v. In Figure 2, $k_d = 4$ and $k_v = 1$. Figure 2a consists of the path of R1 in the xy-plan and the formation at several locations. The curves in the Figures 2b-c are x and y errors of R1, R2 and R3, respectively. In Figure 2b, the error of x is a constant zero because the x coordinate of R1 is selected as the value of the reference projection.

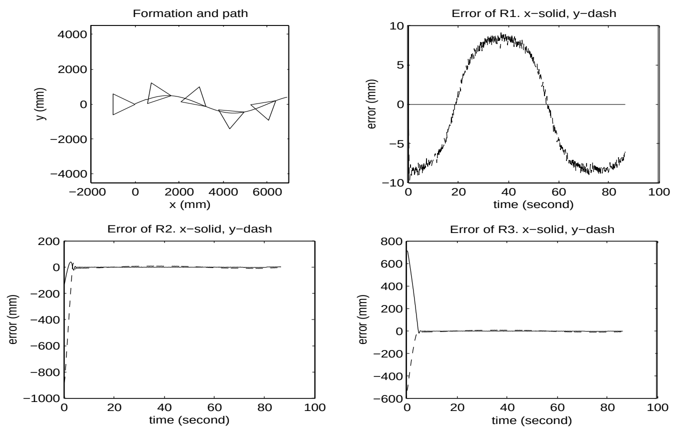

Figure 2: Trajectories and errors

In another experiment, we test the coordination feature of the controller by blocking R1 and observing the reaction of R2 and R3. At about t=32.6s, R1 was stopped. It can be observed in Figure 3b. The error does not change after t=32.6.

Since the reference projection is $s = x_1$, the desired positions of R2 and R3 are computed based on x_1. Therefore, R2 and R3 will finally stop if R1 is stopped. This is shown in the experiment. Another interesting point is that the controller is able to automatically recover the desired formation. In Figure 3b, R1 starts to move at t=87s after the stop. From Figure 3, the other two vehicles recover the desired path automatically. This is because that the coordination is achieved through the reference projection. If x_1 recovers the normal performance, the other vehicles will automatically recover the normal performance. In the entire process, controller re-design or time reset is not involved. The coordination and control are completely autonomous.

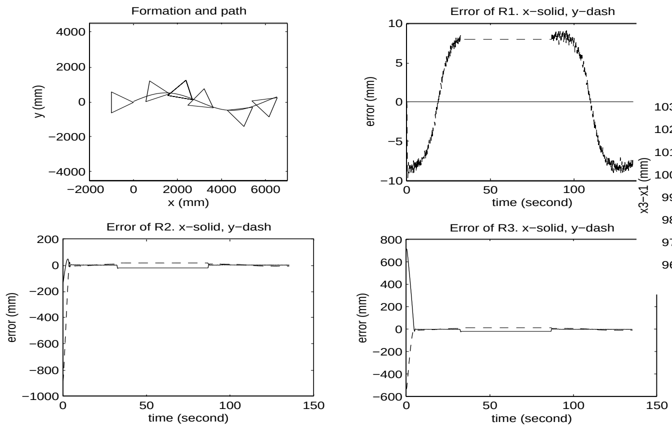

Figure 3: Trajectories and errors

4.2 Simultaneous Movement

In this experiment, we use the same wedge formation as in § 4.1 except that the desired path is the x-axis in the fixed frame. To implement the simultaneous movement strategy, we use the reference projection

$$s = \min\{x_1, x_2 + d_1, x_3 + d_1\}.$$

The initial locations of the robots are (-1200,0), (-1200,1200) and (-1200, -1200) for R1,R2, and R3 respectively. The initial formation is not a wedge. In the experiment, the controller quickly corrected the initial error to form the wedge formation. Then, the formation moved along the x-axis at a speed of 100mm/s. To test the coordination, we stopped R1 during the time interval $[20.2s, 42.9s]$. The other two vehicles stopped automatically because of the specific reference projection used in the controller. In the time interval $[59.4s, 81.1s]$, R2 was stopped. We observed that R1 and R3 automatically stop. During the period of $[96.8s, 125.7s]$, R3 was stopped. The experiment shows that R1 and R2 stop. This proves that the reference projection treats all the vehicles equally. There is no leader or follower. The slow down or stop of any vehicle in the formation will slow down or stop all the other vehicles in the formation. The experimental results are shown in Figure 4. In Figure 4a, the formations are at t = 30, 70 and 100. It shows that the formation is maintained well even when the vehicles experienced unexpected stop. In 4b-c, the curve represents the differences $x_1 - x_2$ and $x_1 - x_3$. If the values of $x_1 - x_2$ and $x_1 - x_3$ equal 1000, the formation is perfect. The formation error shown in Figure 4b-c is due to the unexpected stop of a vehicle in the formation.

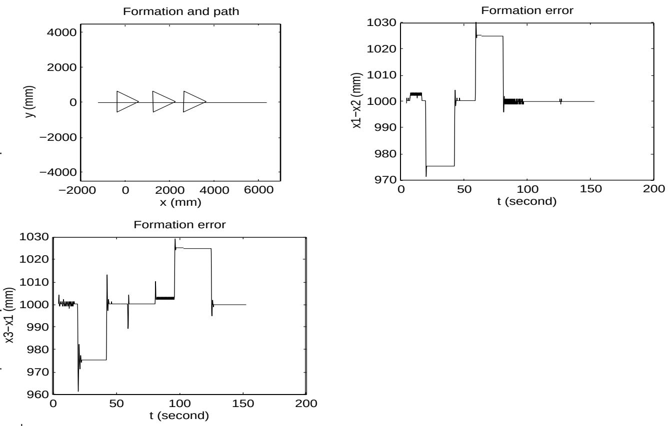

Figure 4: Trajectories and errors

4.3 Series Connection of Formations

In this experiment, the formation is a simple line. Three vehicles are aligned on the x-axis. R2 follows R1 by a distance of $1200mm$. R3 follows R2 by the same distance. In the coordination, the reference of R1, R2 and R3 are defined by

$$s_1 = x_1, \quad s_2 = x_1, \quad s_3 = x_2.$$

In this set of reference projections, R2 follows R1 and R3 follows R2. Therefore, if R2 slows down, it only affects the performance of R3. However, if R1 slows down, both R2 and R3 will slow down. The experiment result is shown in Figure 5. In Figure 5a-b, the curves represent $x_1 - x_2$ and $x_2 - x_3$. In a perfect situation, these values should be $1200mm$. In the experiment, we stop R2 in the time interval $[10.8s, 20.1s]$. Figure 5a shows that the distance

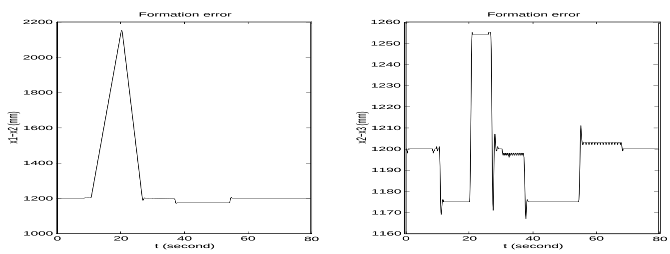

Figure 5: Formation errors

between R1 and R2 increase with constant speed. This is because that R1 is not affected by R2. During the same period of time, the distance between R2 and R3 is stabilized at about $1175mm$ (see Figure 5b). This is because that R3 is the follower of R2. Since R2 is stopped, R3 is stopped too. At $t = 20.1s$, R2 recovers normal performance. It catches up with R1 automatically (Figure 5a). R3 also catches up with R3. The desired formation is maintained. However, Figure 5b shows a relatively large overshoot in the performance of R3 before $x_2 - x_3$ is stabilized. We are developing more sophisticated reference projections to eliminate the overshoot. It will require more information from the sensor. During the time interval $[37.1s, 54.3s]$, R1 is stopped. As shown in Figure 5, both R2 and R3 are stopped. Once R1 recovers its movement, R2 and R3 automatically recover the desired formation.

4.4 Formation Reconfiguration

Easy formation reconfiguration is an important feature for real-life applications. In the following experiment, we show a simple way of formation reconfiguration. In addition to the action reference s, let us take the parameters d_1 and d_2 as additional action references. The new references d_1 and d_2 define the desired formation in the moving frame, as illustrated in § 2.3. These references appear in the controllers of the individual vehicles. In Figure 6, the reference projection of s is the same as in § 4.2. However, the value of d_1 and d_2 are changed during the experiment. At $t = 0$, $d_1 = 1000, d_2 = 600$ for both R2 and R3. The values define a wedge formation. At $t = 20s$, the values of the references are changed to $d_1 = 1200, d_2 = 0$ for R2 and $d_1 = 2400, d_2 = 0$ for R3. Under the new values, the formation is a line with $1200mm$ between consecutive vehicles. In Figure 6, the positions of the three vehicles are shown for $t = 20$, 22.5, 24.5, and 26. It shows the animation of a formation changing from wedge to a line. Similarly, we can easily change the line formation into a wedge formation.

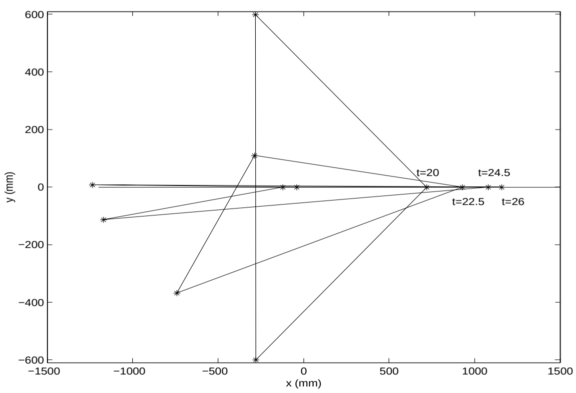

Figure 6: Formation reconfiguration

5 CONCLUSION

The controller design in a perceptive frame for the formation control of multiple vehicles is applied to mobile robots. Simulations and experiments show that the designed controllers are able to coordinate multiple subsystems and drive them move in a given formation. The design algorithm has several advantages. First, the controller is able to follow a variety of coordination strategies in the presence of unexpected event. Changing a coordination strategy does not require major re-planning. The second advantage is its ability of easy system reconfiguration. Changing the formation does not require controller re-design. The third advantage is that the feedbacks of individual vehicles can be designed using almost any trajectory tracking technique that exists in the literature. The controller of the entire formation is an assembly of the individual feedbacks in a perceptive frame.

REFERENCES

Kang, W., N. Xi, and A. Sparks (2000). Theory and applications of formation control in a perceptive referenced frame. *Proc. IEEE Conference on Decision and Control*, Sydney, Australia, December 12-15.

Kang, W., and N. Xi (1999). Non-Time referenced tracking control with application in unmanned vehicle. *Proc. IFAC World Congress of Automatic Control*, Beijing, China, July 5-9.

Kang, W., A. Sparks, and S. Banda (2001). Coordinated Control of Multi-Satellite Systems. *AIAA J. of Guidance, Control, & Dynamics*, Vol **24**, NO. **2**, pp. 360-368.

McInnes, C. R. (1995). Autonomous ring formation for a planar constellation of satellites. *J. Guid. , Contr., and Dynm.*, **Vol. 18**, **NO. 5**, pp. 1215-1217.

Sampei, M., T. Tamura, T. Itoh and M. Nakamichi (1991). Path tracking control of trailer-like mobile robot. *IEEE/RSJ International Workshop on Intelligent Robots and Systems IROS'91*, pp. 193-198, Osaka, Japan.

Tarn, T. J., A.K. Bejczy and Ning Xi (1993). Intelligent Planning and Control for Robot Arms. *Proceedings of the IFAC World Congress*, Sydney, Australia, July 18-23.